Crystal Structures of Tetrakis(4,4′-(2,2-diphenylvinyl)-1,1′-biphenyl)methane: Transmission Electron Microscopy and X-ray Diffraction

C. Y. Yang,[†] Shujun Wang,[‡] Mathew R. Robinson,[‡,§] Guillermo C. Bazan,[‡,§] and Alan J. Heeger*[,†,§,||]

Institute of Polymers and Organic Solids, Department of Chemistry, Materials Department, and Department of Physics, University of California, Santa Barbara, California 93106

Received October 10, 2000. Revised Manuscript Received February 20, 2001

The crystal structures of tiny crystallites (micron to submicron in size) of tetrakis(4,4′-(2,2-diphenylvinyl)-1,1′-biphenyl)methane ($C(DPVBi)_4$) have been investigated by using a combination of transmission electron microscopy (TEM) and X-ray powder diffraction techniques. The crystal structure of as-synthesized $C(DPVBi)_4$ is hexagonal. The lattice parameters are $a = 2.068$ nm and $c = 2.194$ nm with possible space group $P6$. After $C(DPVBi)_4$ was annealed up to 280 °C, the crystal structure converted to a different hexagonal structure with lattice parameters: $a = 2.102$ nm and $c = 3.370$ nm. The possible space group is $P6/m$. The two hexagonal structures correspond to different packing of the individual molecules, which may result in different bulk optical and electronic properties.

Introduction

Tetrahedral molecules that bring together four conjugated fragments in a tetrahedral arrangement are interesting structures in which each molecule is constructed by connection to a nonfluxinal core. This topological feature is expected to inhibit crystallization. The nonparallel arrangement of the individual components should also lead to weaker interchain coupling, thereby increasing the solid-state emission (photoluminescence) quantum yield and utility in light-emitting diodes.[1−4]

In a recent contribution the synthesis of a wide range of tetrahedral molecules that fit the above structural criteria was reported.[5−8] It was found that the length of the tetramer "arms" plays an important role in determining the ability of the bulk to crystallize. For example, while $C(STB)_4$ is a crystalline compound, the tetra(distyrylbenzene)methane derivative $C(^tBuSSB)_4$ is amorphous with a glass transition at ∼175 °C.

In the case of T-4R−OC_6H_{13}, it is possible to cast homogeneous films directly from solution and use these

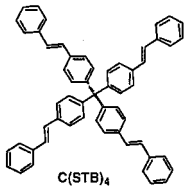

$C(STB)_4$

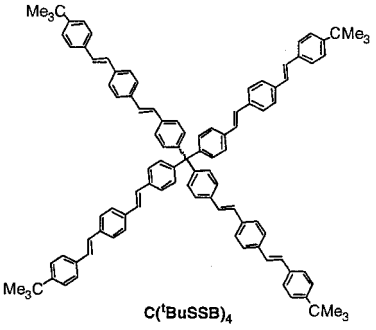

$C(^tBuSSB)_4$

as the electroluminescent layer in organic light-emitting diodes.

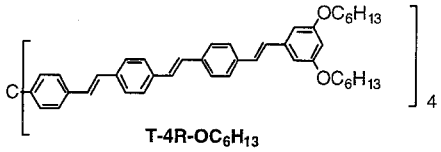

T-4R-OC_6H_{13}

The arms of $C(DPVBi)_4$ have intermediate dimensions. When obtained as a powder from noncoordinating solvents, the material is partially crystalline with tiny crystallites embedded in an otherwise amorphous medium.

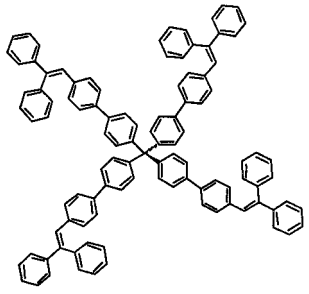

$C(DPVBi)_4$

* To whom correspondence should be addressed.
[†] Institute of Polymers and Organic Solids.
[‡] Department of Chemistry.
[§] Materials Department.
[||] Department of Physics.

(1) Jenekhe, S. A.; Osaheni, J. A. *Science* **1994**, *265*, 765.
(2) Yan, M.; Rothberg, L. J.; Paradimitrakopoulos, F.; Galvin, M. E.; Miller, T. M. *Phys. Rev. Lett.* **1994**, *72*, 1104.
(3) Rothberg, L. J.; Yan, M.; Paradimitrakopoulos, F.; Galvin, M. E.; Kwock, E. W.; Miller, T. M. *Synth. Met.* **1996**, *80*, 41.
(4) Berggren, M.; Dodabalapur, A.; Slusher, R. E.; Bao, Z. *Nature* **1997**, *389*, 466.
(5) Oldham, W. J., Jr.; Lachicotte, R.; Bazan, G. C. *J. Am. Chem. Soc.* **1998**, *120*, 2987, and supplemental material.
(6) Wang, S. J.; Oldham, W. J., Jr.; Hudack, R. A.; Bazan, G. C. *J. Am. Chem. Soc.* **2000**, *122*, 2000.
(7) Johansson, N.; Salbeck, J.; Bauer, J.; Weissortel, F.; Broms, P.; Andersson, A.; Salaneck, W. R. *Adv. Mater.* **1998**, *10*, 1136.
(8) Yu, W. L.; Pei, J.; Huang, W.; Heeger, A. J. *Adv. Mater.* **2000**, *12*, 828.

10.1021/cm001194k CCC: $20.00
Published on Web 06/09/2001

Because the microstructure, or local environment, of oligomers influences greatly the physical properties of the material, it is of interest to understand the intermolecular packing and orientation of the tetrahedral molecules. Unfortunately, large, defect-free crystals suitable for single-crystal X-ray diffraction experiments are not available.

In such partially crystalline organic substances, a combination of TEM and X-ray powder diffraction techniques can be used to determine the crystal structure and hence the molecular packing. TEM gives information on the morphology of the sample and, simultaneously, provides the two-dimensional electron diffraction pattern of microcrystallites (typically microns in size) that are contained within the sample,[9] while the powder X-ray diffraction is sensitive to the overall *d* spacings between crystal planes of the crystallites.[10,11] The crystallographic symmetry can be obtained from the electron diffraction pattern if a crystallite is oriented with its zone axis parallel to the optical axis of the TEM. The symmetry obtained from the electron diffraction pattern corresponds to the symmetry of the crystallite, and hence the symmetry of the molecular packing within the crystallite.[12] Therefore, once the symmetry is known, the three-dimensional crystallographic structure can be constructed by using the X-ray powder diffraction data. Finally, the inferred structure can be verified by using diffraction theory to calculate the *d* spacings between crystalline planes of the model structure[9−12] and compared with the *d* spacings observed in the powder diffraction spectrum.

There is limited structural information available in the literature for tetrahedral oligo(phenylenevinylene) compounds probably because of the absence of large crystals needed for single-crystal diffraction. The crystal structure of tetrastilbenoidmethane, C(STB)$_4$, determined by Warren et al. by using single-crystal X-ray diffraction, is tetragonal with lattice parameters a = 1.75046 nm and c = 0.71921 nm.[5] An isomorphous structure was reported for tetrastilbenyladamantane, Ad(STB)$_4$.[6]

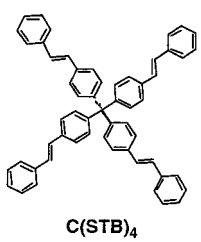

C(STB)$_4$

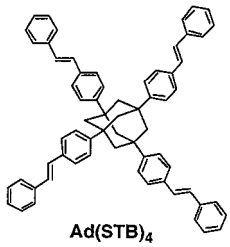

Ad(STB)$_4$

In this report, we demonstrate a methodology for solving the crystal structure of the small and imperfect crystallites (microns in size) of tetrakis(4,4′-(2,2-diphenylvinyl)-1,1′-biphenyl)methane, C(DPVBi)$_4$, by using a combination of TEM and powder X-ray diffraction.

(9) Hirsch, P.; Howie, A.; Nicholson, R. B.; Pashley, D. W.; Whelan, M. J. *Electron Microscopy of Thin Crystals*; Robert E. Krieger Publishing Co.: Huntinton, NewYork, 1977.

(10) Guinier, A. *X-ray Diffraction*; W.H. Freeman and Co.: San Francisco, 1963.

(11) Vainshtein, B. K. *Diffraction of X-rays by Chain Molecules*; Elsevier: Amsterdam, 1966.

(12) Ladd, M. F. C. *Symmetry in Molecules and Crystals*; Halsted Press: New York, 1989.

Experimental Section

The compound, C(DPVBi)$_4$, was synthesized as previously described.[6]

A JEOL 100CX TEM, with accelerating voltage of 100 kV, was used to obtain the morphology and the electron diffraction pattern for both the as-synthesized and annealed samples of C(DPVBi)$_4$. The instrument had to be operated under conditions of minimum dose to avoid damaging the sample by electron irradiation. Because there is no dosimeter equipped in the JEOL 100CX TEM, the minimum dose was obtained by adjusting the size of the electron beam spot (to No. 3), the size of condenser aperture (to No. 2), and the condenser lens current to fully spread the beam. Even under these experimental conditions, there were obvious signs of degradation; that is, the diffraction spots became blurred within several minutes. The data used in the analysis reported here were obtained prior to any indication of degradation; that is, the patterns were taken as soon as they were seen within 1 or 2 min.

To obtain the on-axis diffraction pattern, crystallites with a proper orientation with respect to the TEM beam had to be chosen and/or the sample had to be oriented with respect to the TEM beam. This procedure was difficult and not always successful because the crystallites are damaged under electron irradiation.

A Philips X'pert diffractometer with a power of 40 mA and 45 kV (X-ray wavelength λ = 1.5406 Å) was used for collection of *d* spacings for both of the as-synthesized and the annealed samples of C(DPVBi)$_4$. The scan range $2\theta = 1°-35°$. The scan speed is 0.00057 (°/s).

Thermal properties were studied by using the differential scanning calorimeter (TA DSC-2920) and thermogravimetry analysis instrument (Mettler 851e TGA). The heating and cooling rate were 10 °C/min for both DSC and TGA runs. The purge gas in both DSC and TGA runs was N_2. The annealed sample was prepared in DSC cycle in an aluminum pan, closed by the lid with a weight of 15.4 mg. The TGA sample with a weight of 18.9 mg was heated in an open ceramic crucible.

Results and Discussion

Two different crystal structures were determined: one for the as-synthesized C(DPVBi)$_4$ and one for the sample after annealing up to 280 °C.

(1) Crystal Structure of As-Synthesized Tetrahedral C(DPVBi)$_4$. The morphology of the powder sample, including the size of the crystallites and/or the aggregates, can be seen directly by electron microscopy (Figure 1). In Figure 1, there are larger particles of ∼1-μm size, which were identified as crystallites by electron diffraction. Additionally, smaller particles of ∼1−10-nm size can be observed, which gather in clusters, and in which the tetrahedral molecules may or may not be three-dimensionally ordered.

After a careful search by using the selected area diffraction,[9] the electron diffraction pattern along the principle zone axis of the crystallites has been obtained, as shown in Figure 2a**.** In addition, a different zone axis pattern (Figure 2b) was also obtained from a different crystallite. Figure 2a shows clearly the hexagonal symmetry of the two-dimensional diffraction spots (there are also some irregular diffraction spots that come from imperfections in the crystallite and/or from the adjacent crystallites). Thus, the electron diffraction pattern of Figure 2a demonstrates that, in these crystallites, the molecules pack such that the resulting lattice has hexagonal symmetry. Note that the hexagonal symmetry of the two-dimensional diffraction pattern of Figure 2a could result from either the (0001) plane

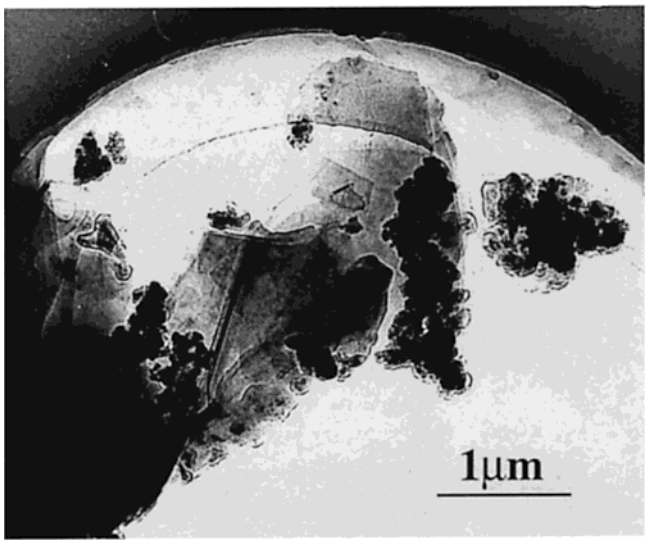

Figure 1. TEM picture showing the morphology of the as-synthesized $C(DPVBi)_4$ sample.

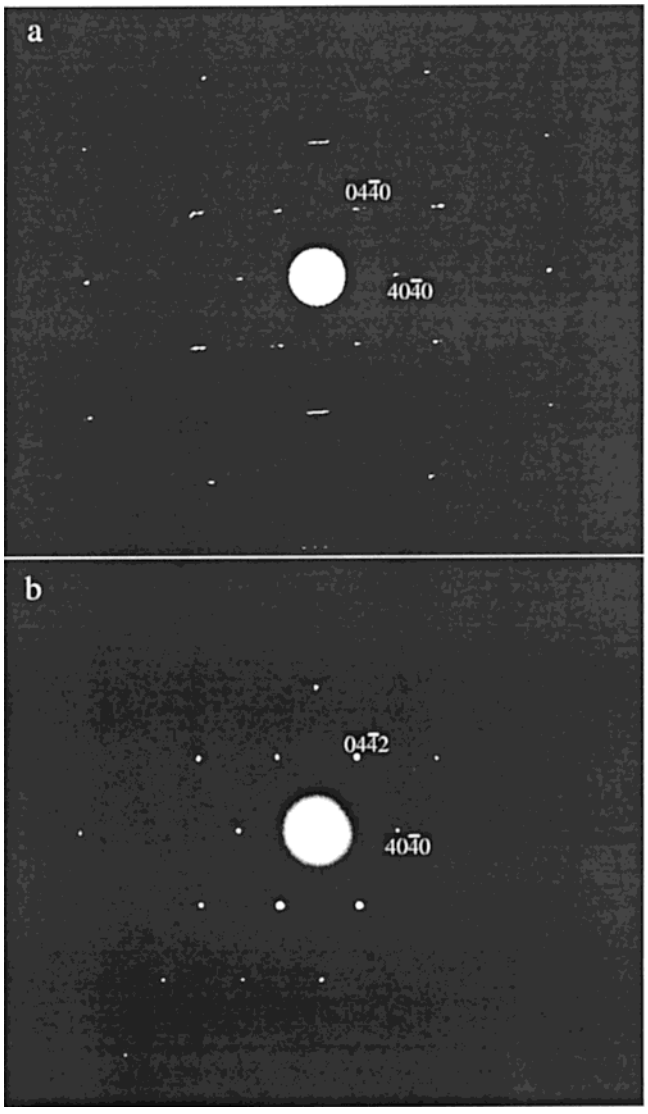

Figure 2. [0001] (a) and [1$\bar{2}$16] (b) zone axis patterns. Figure 2a shows clearly the hexagonal symmetry of the electron diffraction spots.

of a hexagonal crystal system (the rhombohedral lattice in this plane is compatible with that of a hexagonal

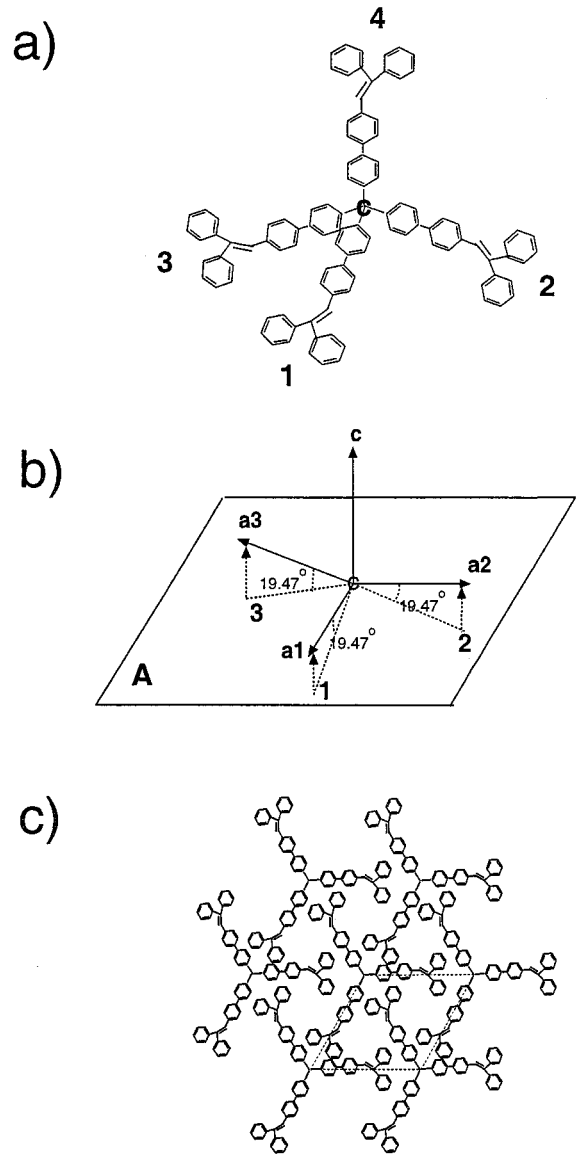

Figure 3. Schematic drawings of the construction of the crystallographic model of as-synthesized $C(DPVBi)_4$. (a) is a three-dimensional construction of the tetrahedral molecule; (b) is the geometry of the construction of the hexagonal axes that is related to (a); (c) is the projection of the molecular packing, showing the hexagonal lattice along the **c** direction.

system)[12] or the (111) plane of a cubic lattice. However, the cubic alternative was excluded because we were able to index all the electron diffraction spots and the X-ray diffraction peaks only in the hexagonal system; see below.

Thus, we consider the possible ways to pack the tetrahedral $C(DPVBi)_4$ in a hexagonal lattice. Assume that a single tetrahedral molecule is sketched in three dimensions with arms 1, 2, 3, and 4, as shown in Figure 3a. For clarity, we simplify every arm of the tetrahedral molecule as a director of the lattice array, and then we have director **c** for arm 4 and the dashed lines 1, 2, and 3 for arms 1, 2, and 3, respectively, as shown in Figure 3b. Further, if we project three dashed lines 1, 2, and 3 up onto plane A, which is normal to **c** and through the molecular center (the core atom of carbon C), then we have the projections **a1**, **a2**, and **a3** in plane A, respectively, as shown in Figure 3b. Thus, we have directors **a1**, **a2**, **a3**, and **c**. The angle between **a1** and **a2**, **a2** and

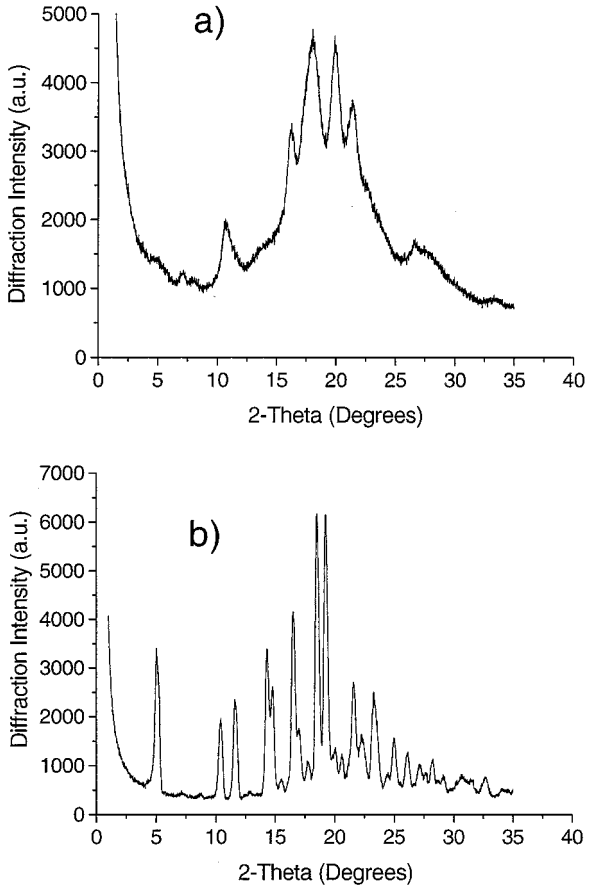

Figure 4. X-ray diffraction spectrums: (a) for as-synthesized and (b) for annealed C(DPVBi)$_4$ samples.

Table 1. *d* Spacings and Indexes of As-Synthesized C(DPVBi)$_4$ from X-ray and Electron Diffraction

no.	$d_{obs} \pm 0.005$ (nm)	relative intensity	$d_{cal} \pm 0.005$ (nm)	*hkil*
1	1.800	9	1.792	$10\bar{1}0$
2	1.314	12	1.388	$10\bar{1}1$
3	1.097	5	1.097	0002
4	0.830	26	0.829	$20\bar{2}1$
5	0.651	11	0.647	$12\bar{3}1$
6	0.551	60	0.549	0004
7	0.492	100	0.497	$13\bar{4}0$
				$21\bar{3}3$
				$11\bar{2}4$
8	0.448	100	0.448	$40\bar{4}0$
9	0.423	31	0.422	$22\bar{4}3$
10	0.414	71	0.415	$04\bar{4}2$
11	0.389	28	0.391	$14\bar{5}0$
12	0.334	11	0.335	$24\bar{6}1$
				$22\bar{4}5$
13	0.321	9	0.322	$15\bar{6}0$
				$12\bar{3}6$
				$50\bar{5}3$
14	0.295	3	0.296	$60\bar{6}1$
				$20\bar{2}7$
				$34\bar{7}0$
			0.295	$13\bar{4}6$
				$20\bar{2}7$
			$20\bar{2}7$	$15\bar{6}3$
			$15\bar{6}3$	
15	0.267	5	0.268	$24\bar{6}5$
				$22\bar{4}7$
			0.267	$14\bar{5}6$
				$25\bar{7}3$
16	0.234	5	0.234	$48\bar{4}4$
				$04\bar{4}8$

a3, and **a3** and **a1**, respectively, is 120°. Eventually, we take these axes **a1**, **a2**, **a3**, and **c** as hexagonal axes. On the basis of this geometry and the hexagonal lattice, it is possible to sketch the molecular packing in projection, as shown in Figure 3c. Figure 3c is the two-dimensional packing skeleton of the tetrahedral molecules of C(DPVBi)$_4$ on the projection plane. Note that the molecules pack in an ordered hexagonal lattice. The arms of one molecule form an angle of approximately 60° with the arms of adjacent molecules, respectively. In other words, the arms are not in parallel packing, and they do not overlap with each other. The sketched rhomboid (dashed line in Figure 3c) is the unit cell in the projection of the hexagonal lattice. Thus, we have constructed the lattice model of the tetrahedral molecular packing based upon the symmetry of the TEM data. However, because this model is only based upon two-dimensional crystallographic information, mainly the symmetry, the data are not sufficient for determining the three-dimensional crystal structure, the lattice parameters. To complete the structural model, it is necessary to use X-ray diffraction data and to verify the inferred structure with simulations.

Figure 4a is a powder X-ray diffraction spectrum of an as-synthesized sample, showing the broad diffraction peaks. These diffraction peaks result from all particles, as shown, for example, in Figure 1. The *d* spacings between crystalline planes, obtained from the X-ray diffraction peaks observed in Figure 4a, are listed in column 2 of Table 1. The X-ray data help in the indexing of the diffraction spots in Figure 2a; the long *d* spacing, $d = 1.80$ nm in column 2 of Table 1, is not observed in the electron diffraction pattern because of the experimental conditions in TEM. Consider, for example, one of the nearest spots in the electron diffraction pattern; the $40\bar{4}0$ as indicated in Figure 2a. The *d* spacing, corresponding to this spot, $d_{40\bar{4}0} = 0.448$ nm, can be obtained directly from the pattern. Then, we can infer that $d_{10\bar{1}0} = 0.448 \text{ nm} \times 4 = 1.792$ nm, which is consistent with the *d* spacing of 1.80 nm obtained from the X-ray diffraction data. Thus, from the diffraction geometry of the hexagonal lattice, we obtain one of the lattice parameters, $a = d_{10\bar{1}0} \times (2/\sqrt{3}) = 1.792 \text{ nm} \times (2/\sqrt{3}) = 2.069$ nm.[11,12] Further, because the angle between the tetrahedral bonds is 109.47°, the angle between the arm 1 (the dashed line 1) and its projection **a**1 (same for angles between the dashed lines 2, 3 and **a2**, **a3**, respectively) is 19.47°, as shown in Figure 3b. Because the lengths of the four arms are identical, then we can calculate $c = \text{a1}/(\cos 19.47°) = a/(\cos 19.47°) = 2.069 \text{ nm}/(\cos 19.47°) = 2.194$ nm, according to the geometry of Figure 3b. Thus, we have obtained the hexagonal cell parameters *a* and *c* from the electron diffraction pattern of Figure 2a by considering the long *d* spacings obtained from the X-ray data.

By defining the unit cell parameters of *a* and *c*, as demonstrated above, we relied on the TEM data of Figure 2, but not on the broad peaks of X-ray diffraction of Figure 3. We use the X-ray data as complementary information to find the low-order reflection (for example, $10\bar{1}0$), that is missed in TEM patterns and that is related to the high-order reflection ($40\bar{4}0$) in Figure 2a. The experimental errors in *d* spacings from the spots are smaller than what would be obtained from the broad peaks in the X-ray diffraction. The accuracy in TEM data, obtained from Figure 2, is $\Delta d_{max} \cong \pm 0.005$ nm.

Finally, we verify the structure by calculating the *d* spacings using this set of hexagonal lattice parameters: $a = 2.068$ nm and $c = 2.194$ nm. The calculated *d* spacings and their indices are listed in columns 4 and 5 of Table 1, respectively. Comparing column 4 and column 2, we can see that the calculated *d* spacings are typically matched with the observed values for the powder sample within experimental error of $\Delta d_{max} \cong \pm 0.005$ nm. There is one exception: the difference between $d_{obs} = 1.314$ nm and $d_{cal} = 1.388$ nm for $10\bar{1}0$ reflection (Table 1) is 0.074 nm and is 1 order bigger than the estimated experimental error of 0.005 nm noted above. This suggests imperfection of the crystalline plane $\{10\bar{1}1\}$ in the small crystallites. Actually, the inaccuracy in *d* spacings due to the imperfect crystalline planes that result in broad and/or weak diffraction peaks does not affect the major characteristic crystalline feature: the hexagonal symmetry unit cell and the molecular packing mode.

In addition to verification of the unit cell, we indexed all electron diffraction spots, shown in Figure 2 for [0001] (a) and $[1\bar{2}16]$ (b) zone axis patterns, by using the set of the hexagonal cell parameters defined above, respectively. (a) and (b) of Figure 2 are closely related. They have a common *a** axis, that is, $[40\bar{4}0]$ direction. As a matter of fact, Figure 2b can be obtained from Figure 2a by rotation of an angle of 19.95°, calculated with the indexes, along the **a*** direction. So we are able to prove once again that the constructed crystal structure is correct. Otherwise, it would not be possible to index the $[1\bar{2}16]$ pattern. Note that the calculated *d* spacings are valid for all equivalent indices, that is, all equivalent crystal planes. Therefore, we have verified that the crystal structure inferred from the data obtained from the as-synthesized tetrahedral $C(DPVBi)_4$ is correct; hexagonal with lattice parameters $a = 2.068$ nm and $c = 2.194$ nm. The only possible space group is $P\bar{6}$, according to the symmetry of the molecular packing, that is, the hexagonal lattice with point group $\bar{6}$, and the extinction rule of diffraction (that is, there seem to be no conditions for *hkil* reflections).[14]

(2) Crystal Structure of Tetrahedral $C(DPVBi)_4$ after Annealing in a DSC Cycle. A similar approach was used to determine the crystal structure of the annealed sample. The morphology and the diffraction pattern of the crystallite taken from TEM are shown in Figure 5. The morphology of a typical crystallite is observed as the large white features with size greater than 5 μm. This morphology is quite different from that of as-synthesized tetrahedral $C(DPVBi)_4$ (Figure 1). The crystallites are significantly larger and better defined than those in the as-synthesized sample. However, they are still not big enough for single-crystal X-ray diffraction.

Unfortunately, it was not possible to obtain the electron diffraction pattern with a principal zone axis (a highest symmetry axis) by TEM because the crystallites were oriented mostly far from the optical axis of the TEM. Before the high-symmetry axis of the crystallite could be reached by rotation in the TEM, the irradiation damaged the crystal. However, we obtained an important electron diffraction pattern with orthogonal symmetry, though it is slightly off-axis, as shown in the inset in Figure 5. This pattern implies that the molecules of tetrahedral $C(DPVBi)_4$ must pack in an

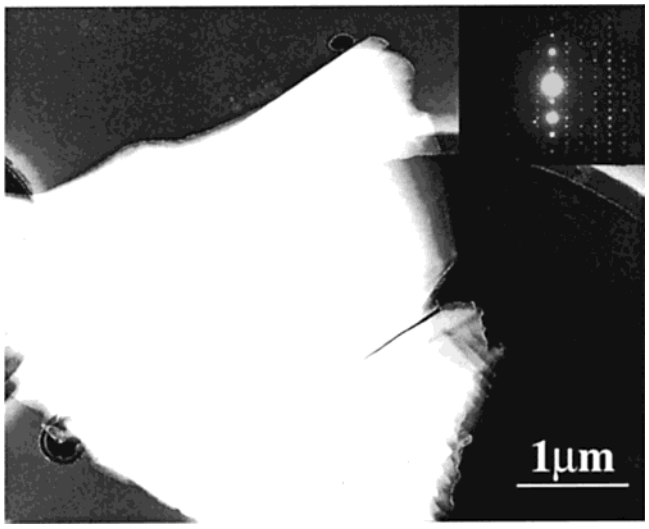

Figure 5. TEM pictures, showing the morphology and the diffraction pattern (the insert) of a typical crystallite of the annealed $C(DPVBi)_4$.

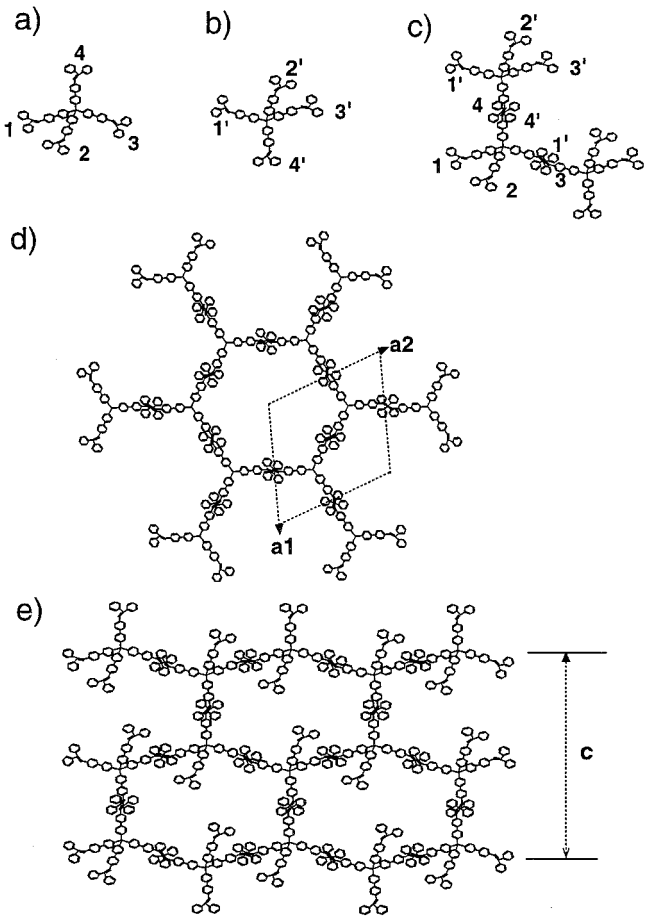

Figure 6. Schematic drawings of a crystallographic construction of the unit cell of the annealed $C(DPVBi)_4$ sample: (a) up-sit molecule; (b) down-sit molecule; (c) the nematic and/or parallel packing of the arms of the adjacent molecules; (d) the molecular packing, viewed from the direction parallel to the **c** axis; (e) the molecular packing viewed from the direction perpendicular to the **c** axis.

(13) Okamoto, P. R.; Thomas, G. *Phys. Stat. Sol.* **1968**, *25*, 81.
(14) *The International Tables for Crystallography*; Hahn, T., Ed.; D. Reidel Publishing Co.: Dordrecht, 1983; Vol. 4, Space-Group Symmetry.

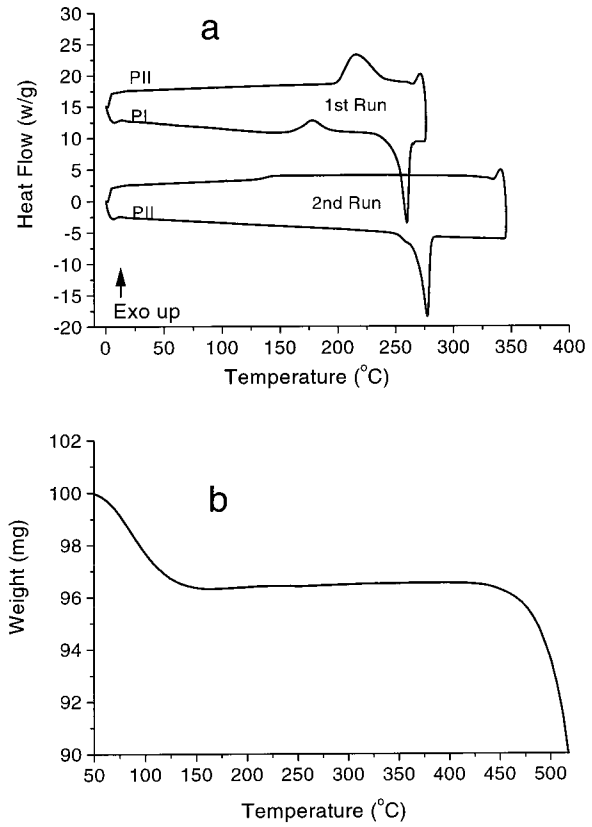

Figure 7. Thermal properties of the tetrahedral C(DPVBi)$_4$. (a) are DSC curves of 2 runs: first run, showing the melting point of 260 °C and the crystallization point of 216 °C; second run, showing the melting point of 278 °C. (b) is the TGA curve, showing the decomposition point that is beyond 400 °C.

orthogonal lattice in this plane. Keeping this orthogonal lattice (electron diffraction pattern) in mind, we construct the molecular model of the structure as follows. Consider a tetrahedral molecule of C(DPVBi)$_4$ with arm 4 up and arms 1, 2, and 3 are 109.47° apart from arm 4 and from each other (Figure 6a). Assume that a second molecule turns upside down from the position of first molecule, that is, from Figure 6a to Figure 6b and hence arm 4 to arm 4′. Thus, the first and second molecules are going to "shake hands" as they approach one another, that is, arms 4 and 4′ and arms 3 and 1′ go into a nematic and/or parallel packing, respectively, as shown in Figure 6c. This happens because the thermal energy renders the molecules more mobile, especially upon melting (the melting point is 260 °C; see Figure 7a). This nematic, and/or parallel packing of the arms, seems sterically and energetically favorable in the context of the molecular geometry. Furthermore, if all arms are going to a nematic or parallel packing, then we obtain the skeletons shown in Figure 6d and Figure 6e. Figure 6d shows this skeleton, viewed from the direction parallel to the up and down arm packing, that is, the direction parallel to the arms 4 and 4′ packing. Figure 6e is the skeleton viewed from the direction perpendicular to arms 4 and 4′ packing. Thus, it is seen clearly that the tetrahedral molecules pack once again in a hexagonal structure. Figure 6d and 6e are projections along and perpendicular to the **c** axis, respectively. The dashed lines in Figure 6d and Figure 6e are hexagonal axes **a** (unit cell projection) and **c**, respectively. This hexagonal lattice is totally different from

Table 2. *d* Spacings and Indexes of Annealed C(DPVBi)$_4$ from X-ray and Electron Diffraction

no.	$d_{obs} \pm 0.005$ (nm)	relative intensity	$d_{cal} \pm 0.005$ (nm)	*hkil*
1	1.685	34	1.685	0002
2	1.233	1	1.237	10$\bar{1}$2
3	1.027	1	1.051	11$\bar{2}$0
			1.003	11$\bar{2}$1
4	0.910	1	0.910	20$\bar{2}$0
5	0.847	25	0.843	0004
6	0.765	34	0.767	11$\bar{2}$3
			0.765	10$\bar{1}$4
7	0.690	2	0.688	12$\bar{3}$0
8	0.617	52	0.618	20$\bar{4}$4
9	0.598	38	0.597	30$\bar{3}$1
10	0.570	6	0.571	30$\bar{3}$2
11	0.534	54	0.534	30$\bar{3}$3
			0.533	12$\bar{3}$4
12	0.525	21	0.525	22$\bar{4}$0
13	0.498	11	0.502	22$\bar{4}$2
			0.499	13$\bar{4}$1
14	0.478	99	0.476	20$\bar{2}$6
15	0.455	100	0.455	40$\bar{4}$0
			0.451	40$\bar{4}$1
16	0.442	17	0.446	22$\bar{4}$4
			0.439	40$\bar{4}$2
17	0.430	15	0.433	13$\bar{4}$4
18	0.411	40	0.414	23$\bar{5}$1
19	0.397	20	0.397	14$\bar{5}$0
			0.395	14$\bar{5}$1
20	0.382	37	0.387	14$\bar{5}$2
21	0.364	8	0.364	50$\bar{5}$0
22	0.355	20	0.359	14$\bar{5}$4
			0.356	50$\bar{5}$2
23	0.339	13	0.342	24$\bar{6}$1
			0.337	24$\bar{6}$2
24	0.327	11	0.329	24$\bar{6}$3
			0.327	15$\bar{6}$0
			0.325	15$\bar{6}$1
25	0.321	8	0.323	13$\bar{4}$8
			0.321	15$\bar{6}$2
			0.320	50$\bar{5}$5
26	0.315	13	0.318	24$\bar{6}$4
			0.315	23$\bar{5}$7
			0.314	15$\bar{6}$3
27	0.305	7	0.306	14$\bar{5}$7
			0.305	15$\bar{6}$4
			0.303	60$\bar{6}$0
28	0.290	4	0.291	25$\bar{7}$0
			0.290	25$\bar{7}$1
			0.289	34$\bar{7}$3

that described above for the as-synthesized sample. In this structure, the four arms of the adjacent molecules are all nematic and parallel ordered with respect to each other, while in the previous structure the four arms of the adjacent molecules form angles of 60° to each other.

Note that Figure 6e shows an orthogonal lattice, which should result in the same orthogonal lattice in reciprocal plane. This corresponds to the orthogonal electron diffraction pattern (the inset in Figure 5) mentioned above. Thus, if we assume that this diffraction pattern corresponds to the (10$\bar{1}$0)* reciprocal plane, then we can determine the lattice parameters: $a =$ 2.102 nm and $c = 3.370$ nm directly, using the horizontal and vertical diffraction spot arrays.

Finally, to verify this hexagonal structure, we have to match all X-ray diffraction data with this set of parameters. Figure 4b is the X-ray diffraction spectrum of the annealed sample. All the observed *d* spacings from Figure 4b are listed in column 2 of Table 2. Comparing Figure 4b to Figure 4a, it is seen that the spectrum in Figure 4b is quite different from that in Figure 4a, not

only in the numbers and sharpness but also in the positions of the peaks. This means that the thermal effect on tetrahedral C(DPVBi)$_4$ results not only in the growth of the large crystallites but also in a different crystal structure. This result is consistent with the TEM results: two different structures are obtained from Figure 2 and Figure 5. The calculated *d* spacings and indices are listed in columns 4 and 5 of Table 2 by using the set of lattice parameters determined from the electron diffraction pattern. The calculated *d* spacings are all in good agreement with the observed ones with the experimental error in *d* spacings less than 0.005 nm. Only for the $d_{obs} = 1.27$ nm (No. 3 in Table 2) the error seems more than 0.005 nm; however, this is due to the overlap of the reflections of $11\bar{2}0$ and $11\bar{2}1$, as seen in Table 2. Hence, we have successfully indexed all the X-ray diffraction peaks, and we have verified a second tetrahedral molecular packing as well as the crystal structure of C(DPBi)$_4$ in the sample, annealed in DSC up to 280 °C. The structure is hexagonal, with cell parameters $a = 2.102$ nm and $c = 3.37$ nm. The possible space group is $P6/m$.

Finally, the existence of two crystal structures of the tetrahedral C(DPBi)$_4$ determined above obviously shows the polymorphism of tetrahedral C(DPBi)$_4$, consistent with the DSC data. The DSC curves, Figure 7a, show that the melting point is 260 °C and the crystallization point is 216 °C, if the sample is heated to 280 °C in the first run. However, the melting point becomes 278 °C shown in the second run, upon heating to 350 °C. Thus, after the sample was heated to 280 °C and cooled to room temperature, the phase changed from α form (indicated in Figure 7a as PI) of as-synthesized powder to β form (indicated in Figure 7a as PII) of the annealed sample. The melting points for α and β forms are 260 and 278 °C, respectively. The TGA shows that the sample is quite stable, with decomposition only at temperatures greater than 400 °C (Figure 7b). Thus, the sample does not degrade when heated to 280 °C in a DSC run under N_2 gas purge. Therefore, the structural phase transition from α to β occurs without degradation or decomposition. We will discuss the phase transition of tetrahedral C(DPVBi)$_4$ in detail, including the exothermal peak at (150−170) °C, elsewhere.

In conclusion, the crystal structure of tiny crystallites of C(DPVBi)$_4$, too small for single-crystal X-ray diffraction and embedded in an amorphous medium, has been determined by a combination of TEM and X-ray diffraction. The crystal structure of C(DPVBi)$_4$, as-synthesized powder, is hexagonal. The lattice parameters are $a = 2.069$ nm and $c = 2.194$ nm. The possible space group is $P\bar{6}$. Thermal annealing above the melting point results in a phase transition to another hexagonal structure with lattice parameters $a = 2.102$ nm and $c = 3.370$ nm and with possible space group $P6/m$. Two crystal structures (α and β forms) correspond to two different molecular packings of the individual C(DPVBi)$_4$ molecules. In one, the arms of the adjacent molecules form 60° to the arms from the neighbors, while in the other the arms of the adjacent molecules are in nematic and parallel order relative to each other. This different molecular packing may result in different optical and electronic properties.

Acknowledgment. This work was supported by the N00014-91-J-1235 and the MRL Program of the National Science Foundation under Award DMR96-32716.

CM001194K